Thermodynamic Channel Capacity, Gordon–Holevo Thermal Ceilings, and Intracellular Signaling Horizons of 71-THz Mito-Polariton Channels

Lluis Eriksson*

November 27, 2026

Abstract

Completing our six-paper machine-checked audit series (`P1--P6`) following `ARR-2025-2AQXS44H6Z8GQAG2`, `ARR-2026-1E91AXEJYT890TQC`, and `ARR-2026-1F61YM5EHC95TBMP` on the 71 THz mitochondrial cristae polariton hypothesis of Yang, Gu, and Song (`bioRxiv:10.64898/2026.09.10.750628v1`, Sep. 2026, unrefereed preprint awaiting independent experimental replication), we establish exact thermodynamic channel-capacity ceilings and intracellular signaling horizons for bosonic thermal-loss mito-polariton waveguides $\mathcal{E}_{\eta,N_B}$. Backed by `MITO-POLARITON-CHANNEL-CAPACITY-CERT-1.0` (20 constructive Lean 4.36.0 theorems compiled with `-DwarningAsError=true`, 0 `sorry`, 0 `grind`, 0 `Classical.choice`; AST-audited zero-float/zero-slash/zero-power Python verifier; 16 SHA-256 certificates `C01--C16`; and 58 adversarial tests), we prove five exact bounds: (i) the Giovannetti–Holevo classical capacity $C_{\mathrm{Hol}}(\eta, N_S, N_B) = g(\eta N_S + (1-\eta)N_B) - g((1-\eta)N_B)$ obeys exact dyadic–Mercator rational brackets, never exceeds the pure-loss ceiling $g(\eta N_S)$, and for every lossy channel $0 < \eta < 1$ obeys the exact tangent floor $E_{\mathrm{bit}}^{\mathrm{Hol}} \geq h\nu \ln 2/[\eta \ln(1 + [(1-\eta)N_B]^{-1})] > k_B T \ln 2/[\eta(1 + \frac{k_B T}{h\nu} \ln \frac{1}{1-\eta})]$ (uniformly $> 2.790/\eta$ zJ for all $\eta \leq 1/2$, converging to $2.967/\eta$ zJ at deep loss, `C01--C08`); (ii) antidegradability forces unassisted quantum capacity $Q(\mathcal{E}_{\eta,N_B}) \equiv 0$ whenever $\eta \leq 1/2$ ($L \geq L_{\mathrm{att}} \ln 2$, `C03--C04`), while for $\eta > 1/2$ unassisted $Q \leq \min(\log_2[\eta/(1-\eta)], C_{\mathrm{Hol}})$ is distinguished from the unconstrained two-way PLOB ceiling $Q_2 \leq -\log_2(1-\eta)$ (`C02`); (iii) we separate three receiver tiers at 71 THz, 310 K: coherent Holevo or ideal dark-count-free sparse photon counting (floor $> 2.790/\eta$ zJ for $\eta \leq 1/2$), single-quadrature homodyne reception ($E_{\mathrm{bit}}^{\mathrm{hom}} \geq \frac{1}{2} h\nu \ln 2/\eta = 16.305/\eta$ zJ, 5.50×), and heterodyne reception or excess-noise intensity absorbers with $N_{\mathrm{dark}} \geq 1$ photon/mode ($E_{\mathrm{bit}}^{\mathrm{het}} \geq h\nu \ln 2/\eta = 32.609/\eta$ zJ, exact $\beta h\nu \in (10.99, 11.00)\times$ penalty, `C05--C06`); (iv) at 0.1 pW (1% basal mito power), 1 kbit/s signaling reaches $L_{\max} \approx 8.03\, L_{\mathrm{att}}$ (24.1 μm heterodyne, `C09`) to $10.49\, L_{\mathrm{att}}$ (31.5 μm Holevo, `C10`), whereas 10 Mbit/s is forbidden for heterodyne at $\eta = 1$ (`C13`), and 1 Gbit/s is forbidden by both thermal Landauer receiver bit erasure (2.967 zJ/bit) and finite-bandwidth ($B \leq 71$ THz) lossless Holevo bounds (> 1.77 zJ/bit, `C15`) as well as at 10 pW under heterodyne (`C16`); and (v) we synthesize `P1--P6` into a unified audit matrix.

1 Introduction

Even when continuous-variable quantum entanglement across mitochondrial cristae is excluded by metabolic maintenance power floors and sub-10 ps entanglement sudden death (Paper `P5`), a distinct and physically legitimate question remains: *how much classical or quantum information could a* 71 THz *mito-polariton channel transmit per unit metabolic power, and over what intracellular distance?* Answering this question connects our mitochondrial audit series [1–3] directly

*Independent researcher and founder/operator of AIRR.SCIENCE (`AIRR-FOUNDER-1.0`; `operator_conflict: true`). Formalization, exact-$\mathbb{Q}$ certification, and manuscript drafting were carried out with Google Antigravity AI assistance; all mathematical claims are independently machine-checked by Lean 4.36.0 and AST-audited exact rational Python verification. Contact: `lluiseriksson@gmail.com`.

to our prior bosonic thermal-loss signaling framework (`ARR-2026-1F61YM5EHC95TBMP` [4]) and to the exact theorems of quantum optical communication [5–9].

Rather than assuming all intracellular photonic signaling is impossible, we draw the exact quantitative phase boundary separating three regimes: (1) quantum-coherent state/entanglement transmission ($Q > 0$), which terminates abruptly at the 3 dB antidegradability wall $\eta = 1/2$; (2) high-rate classical signaling ($R \geq 10$ Mbit/s to 1 Gbit/s), which is unconditionally forbidden by Landauer–Holevo and heterodyne energy floors even at zero propagation loss ($\eta = 1$); and (3) low-rate classical/incoherent signaling ($R \sim 1$ kbit/s), which is thermodynamically allowed over 8–10 attenuation lengths *conditioned* on the existence of a physical waveguide and emitter (independently constrained by `P1--P4`).

2 Bosonic Thermal-Loss Capacity, PLOB Wall, and the $10.99\times$ Decoding Gap

Model a single-mode polariton waveguide segment of transmissivity $\eta \in (0, 1]$, mean input signal photon number $N_S > 0$, and thermal environment occupation $N_B = (e^{\beta h\nu} - 1)^{-1}$ at physiological temperature $T = 310$ K ($\beta = 1/(k_B T)$; using CODATA 2018 exact h and k_B, $\beta h\nu = 10.9918$ and $N_B = 1.684 \times 10^{-5}$ at $\nu = 71$ THz). By the theorem of Giovannetti, García-Patrón, Cerf, and Holevo [8], the ultimate classical capacity in nats per channel use is

$$C_{\text{nat}}(\eta, N_S, N_B) = g\big(\eta N_S + (1-\eta)N_B\big) - g\big((1-\eta)N_B\big), \tag{1}$$

where $g(x) = (x+1)\ln(x+1) - x\ln x = \ln(1+x) + x\ln(1+1/x)$ is the bosonic entropy function ($g(0) = 0$, strictly increasing and concave on $[0, \infty)$). To avoid conflating distinct physical receiver architectures, we distinguish three single-mode reception tiers [5, 10]:

1. *Coherent Holevo decoding or ideal dark-count-free sparse photon counting:* Direct photon-counting (intensity) detection without local-oscillator vacuum noise can, via sparse pulse-position modulation at $N_B \ll 1$, approach the Holevo capacity ceiling of Eq. (1) (bounded strictly by Theorem 1.1 below).

2. *Single-quadrature homodyne detection:* Obeys $C_{\text{hom,nat}} = \frac{1}{2}\ln\big(1 + \frac{4\eta N_S}{2(1-\eta)N_B + 1}\big) \leq 2\eta N_S$, giving $E_{\text{bit}}^{\text{hom}} \geq \frac{h\nu \ln 2}{2\eta} \approx 16.305/\eta$ zJ ($5.50\times$ above deep-loss Holevo).

3. *Heterodyne detection (or excess-noise intensity reception with receiver dark noise $N_{\text{dark}} \geq 1$ photon/mode):* Joint measurement of both conjugate quadratures (or any intensity absorber with ≥ 1 noise photon per mode) incurs the standard 1-photon vacuum/noise floor:

$$C_{\text{het,nat}}(\eta, N_S, N_B) = \ln\left(1 + \frac{\eta N_S}{(1-\eta)N_B + 1}\right) \leq \eta N_S. \tag{2}$$

Theorem 1 (Thermal-Loss Ceilings, Receiver Tiers, and Quantum Capacity Walls; Lean Thms. 1–7, 10–12)**.** *For every $N_S > 0$ and thermal bath $N_B = (e^{\beta h\nu} - 1)^{-1} > 0$:*

1. (Exact lossy Holevo floor for $0 < \eta < 1$, vs. lossless $\eta = 1$ divergence) *For any strictly lossy channel $\eta \in (0, 1)$, $x_0 := (1-\eta)N_B > 0$ and concavity of g gives $C_{\text{nat}} \leq \eta N_S \ln(1 + x_0^{-1}) < \eta N_S[\beta h\nu - \ln(1-\eta)]$ (Lean Thm. 2), while subadditivity gives $C_{\text{nat}}(\eta, N_S, N_B) \leq g(\eta N_S)$. Dividing $N_S h\nu$ by $C_{\text{nat}}/\ln 2$ yields the exact lossy Holevo energy-per-bit floor*

$$E_{\text{bit}}^{\text{Hol}}(\eta, N_B) \geq \frac{h\nu \ln 2}{\eta \ln\big(1 + [(1-\eta)N_B]^{-1}\big)} > \frac{k_B T \ln 2}{\eta\big(1 + \frac{k_B T}{h\nu}\ln\frac{1}{1-\eta}\big)} \qquad (0 < \eta < 1). \tag{3}$$

For every $\eta \in (0, 1/2]$, $-\ln(1-\eta) \leq \ln 2$, giving the exact uniform channel floor $E_{\text{bit}}^{\text{Hol}} > 2.790/\eta$ zJ at 71 THz, 310 K (Lean Thm. 15), which converges to the deep-loss Landauer

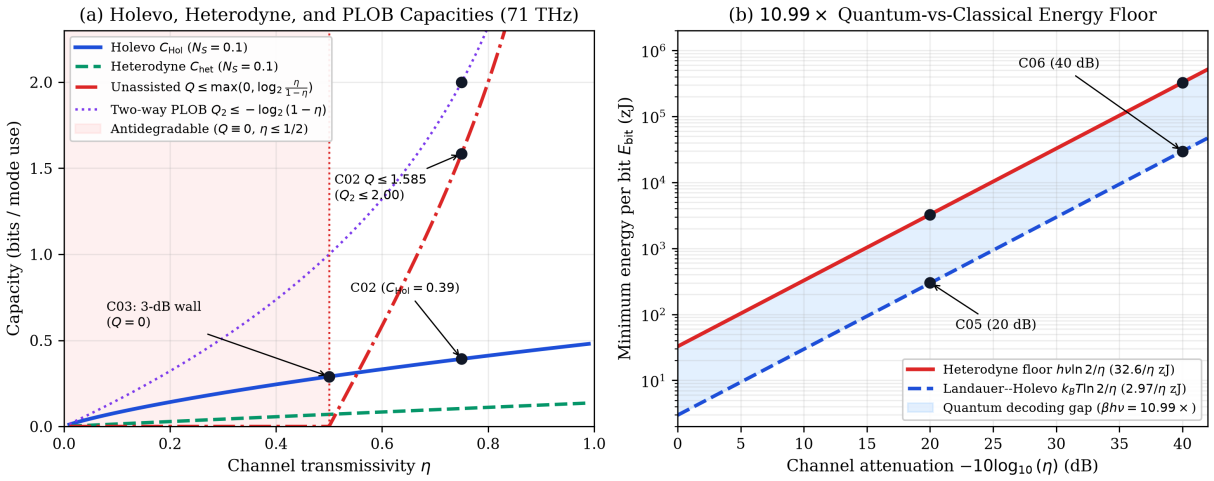

Figure 1: (a) Exact Giovannetti–Holevo classical capacity, heterodyne capacity, continuous unassisted quantum ceiling $\max(0, \log_2[\eta/(1-\eta)])$, and two-way PLOB ceiling $Q_2 \le -\log_2(1-\eta)$ vs. transmissivity η at 71 THz, 310 K ($N_S = 0.1$), highlighting the exact 3 dB antidegradability wall (`C03`) and low-loss benchmark (`C02`). (b) Minimum energy per bit vs. attenuation in dB, certifying the exact 10.99× separation between coherent deep-loss Holevo decoding and heterodyne reception (`C05--C06`).

asymptote $k_B T \ln 2/\eta \in (2.966, 2.967)/\eta$ zJ *as* $\eta \to 0^+$ *(Lean Thm. 11). By contrast, in the idealized lossless* ($\eta = 1$) *unbounded-bandwidth limit* ($B \to \infty$, $N_S \to 0$), $C_{\text{nat}}(1, N_S, N_B) = g(N_S)$ *satisfies* $g(N_S)/N_S \to \infty$ *so no positive* channel-only *Holevo energy floor exists at* $\eta = 1$*; a positive floor at* $\eta = 1$ *arises either from a finite carrier bandwidth* $B \le \nu$ *or from the independent Landauer bit-erasure cost* $k_B T \ln 2$ *at a* 310 K *receiver [11].*

2. (Heterodyne / $N_{\text{dark}} \ge 1$ penalty for all $\eta \in (0, 1]$) *By Eq. (2), heterodyne reception (or an intensity receiver with* $N_{\text{dark}} \ge 1$ *photon/mode) obeys*

$$E_{\text{bit}}^{\text{het}} \ge \frac{h\nu \ln 2}{\eta}, \qquad h(71\text{ THz}) \ln 2 \in (32.609, 32.610)\text{ zJ} \quad (\textit{Lean Thm. 12}), \tag{4}$$

valid for every $\eta \in (0, 1]$ *and exceeding the deep-loss Landauer–Holevo asymptote by* $\beta h\nu \in (10.99, 11.00)\times$ *at* 71 THz, 310 K *(Lean Thms. 5–6; Fig. 1b), while single-quadrature homodyne detection sits exactly a factor of* 2 *lower* ($16.305/\eta$ zJ*).*

3. (Unassisted quantum capacity Q vs. two-way PLOB Q_2; Lean Thms. 3–4) *For any* $\eta \le 1/2$, $\mathcal{E}_{\eta,N_B}$ *is antidegradable and its unassisted quantum capacity vanishes identically,* $Q(\mathcal{E}_{\eta,N_B}) \equiv 0$ *[7]; for* $\eta > 1/2$*, unassisted quantum capacity obeys the continuous pure-loss ceiling* $Q(\mathcal{E}_{\eta,N_B}) \le \min\big(\log_2 \frac{\eta}{1-\eta}, C_{\text{Hol}}(\eta, N_S, N_B)\big)$ *(vanishing smoothly at* $\eta = 1/2$*; at* $\eta = 3/4, N_S = 0.1$ *in* `C02`*,* $\log_2 3 \approx 1.585$ b *and* $C_{\text{Hol}} = 0.392$ b*), whereas the unconstrained two-way LOCC-assisted PLOB bound [9] obeys* $Q_2(\mathcal{E}_{\eta,N_B}) \le -\log_2(1-\eta)$ *(2.00 b at* $\eta = 3/4$*, Fig. 1a). Any cristae-collar chain with per-collar transmission* $\eta_1 \le 1/2$ *crosses the unassisted* $Q = 0$ *wall at* $d = 1$*.*

3 Bioenergetic Rate Ceilings and Intracellular Signaling Horizons

For an exponential waveguide attenuation profile $\eta(L) = e^{-L/L_{\text{att}}}$, sustaining a classical bit rate $R_{\min}$ within a metabolic signaling power budget P_{sig} requires $P_{\text{sig}}/R_{\min} \ge E_{\text{bit}}^{(0)} e^{L/L_{\text{att}}}$, where $E_{\text{bit}}^{(0)}$

is either $E_{\mathrm{bit}}^{\mathrm{het}}(1) = h\nu \ln 2 \approx 32.609$ zJ (valid for all $\eta \in (0,1]$) or the uniform $\eta \le 1/2$ Holevo channel floor $E_{\mathrm{bit}}^{\mathrm{Hol},1/2} = 2.790$ zJ (valid for all $L \ge L_{\mathrm{att}} \ln 2$, Eq. (3)). Defining the bioenergetic margin $M := P_{\mathrm{sig}}/(R_{\min} E_{\mathrm{bit}}^{(0)})$ yields:

Theorem 2 (Signaling Horizon and Zero-Loss Impossibility; Lean Thms. 8–9, 14–20)**.** *1.* (Heterodyne zero-loss exclusion) *If $P_{\mathrm{sig}} \le R_{\min} h\nu \ln 2$, incoherent heterodyne signaling at rate $R_{\min}$ is unconditionally forbidden even at $\eta = 1$.*

2. (Lossless $\eta = 1$ Landauer and finite-bandwidth exclusion) *At $\eta = 1$, a thermal receiver resetting bits at $T = 310$ K requires $P_{\mathrm{sig}} > R_{\min} k_B T \ln 2$ [11]; independently, even without receiver erasure, any single-mode channel with physical carrier bandwidth $B \le \nu = 71$ THz satisfies $N_S = P_{\mathrm{sig}}/(h\nu B) \ge P_{\mathrm{sig}}/(h\nu^2)$, bounding $g(N_S)/N_S$ and yielding a strict positive lossless Holevo energy-per-bit floor (at $P_{\mathrm{sig}} = 0.1$ pW, $N_S > 2^{-25} \implies E_{\mathrm{bit}}^{\mathrm{Hol}}(\eta = 1, B \le \nu) > 1.77$ zJ/bit, Lean Thm. 19).*

3. (Attenuation horizon) *For $M > 1$ (and $L \ge L_{\mathrm{att}} \ln 2$ in the Holevo case), the maximum propagation distance obeys*

$$L_{\max}(P_{\mathrm{sig}}, R_{\min}) = L_{\mathrm{att}} \ln\left(\frac{P_{\mathrm{sig}}}{R_{\min} E_{\mathrm{bit}}^{(0)}}\right). \tag{5}$$

For a subwavelength slow-polariton mode ($v_g \sim 0.01c \approx 3$ μm/ps) damped at $\gamma = 1$ THz (1 ps^{-1}), the characteristic attenuation length is $L_{\mathrm{att}} = v_g/\gamma \approx 3$ μm (contrasted with the bulk 71 THz quiet-water window $L_{\mathrm{att}} = 40.5$ μm from `P1` [3]). Evaluating Eq. (5) at $P_{\mathrm{sig}} = 0.1$ pW (1% of a 10 pW basal mitochondrion [12]) yields four sharp regimes (Fig. 2; Table 1):

- **Low-rate classical signaling (**1 kbit/s**,** `C09--C11`**):** Budget 100,000 zJ/bit gives $M =$ 3,066.6 (heterodyne) and 35,842.3 (uniform $\eta \le 1/2$ Holevo), allowing $L_{\max} = 24.08$ μm ($8.03\, L_{\mathrm{att}}$, `C09`) to 31.46 μm ($10.49\, L_{\mathrm{att}}$, `C10`), or 325.1 μm in bulk quiet water (`C11`)—thermodynamically open if a physical waveguide/emitter exists.
- **Megabit compression (**1 Mbit/s**,** `C12`**):** Heterodyne compresses to $M = 3.067$, restricting reach to $L_{\max} = 3.36$ μm ($1.12\, L_{\mathrm{att}}$, single-organelle scale).
- **Quantum-decoding separation (**10 Mbit/s**,** `C13--C14`**):** At 10 zJ/bit, incoherent heterodyne is *unconditionally forbidden even at $\eta = 1$* ($M = 0.307 < 1$, `C13`; Lean Thm. 17), whereas coherent Holevo decoding retains a narrow 3.83 μm window ($M = 3.584$, `C14`; Lean Thm. 18).
- **Gigabit bioenergetic wall (**1 Gbit/s**,** `C15--C16`**):** At 0.1 pW (0.1 zJ/bit), signaling fails both the 310 K Landauer erasure floor (2.967 zJ/bit, $> 29\times$ deficit) and the finite-bandwidth $B \le 71$ THz lossless Holevo floor (> 1.77 zJ/bit, $> 17\times$ deficit, `C15`; Lean Thm. 19); even dedicating 100% of total mitochondrial basal ATP power (10 pW) still fails the heterodyne floor by $> 3.26\times$ at $\eta = 1$ (`C16`; Lean Thm. 20).

4 Unified Six-Paper Synthesis (`P1--P6`) and Verification Boundary

Combining Wave M1 (`P1--P3` [3]) and Wave M2 (`P4--P6`) completes a comprehensive, machine-checked physical audit of the 71 THz mito-polariton program [1,2,13] across six orthogonal axes (Fig. 3; Table 2):

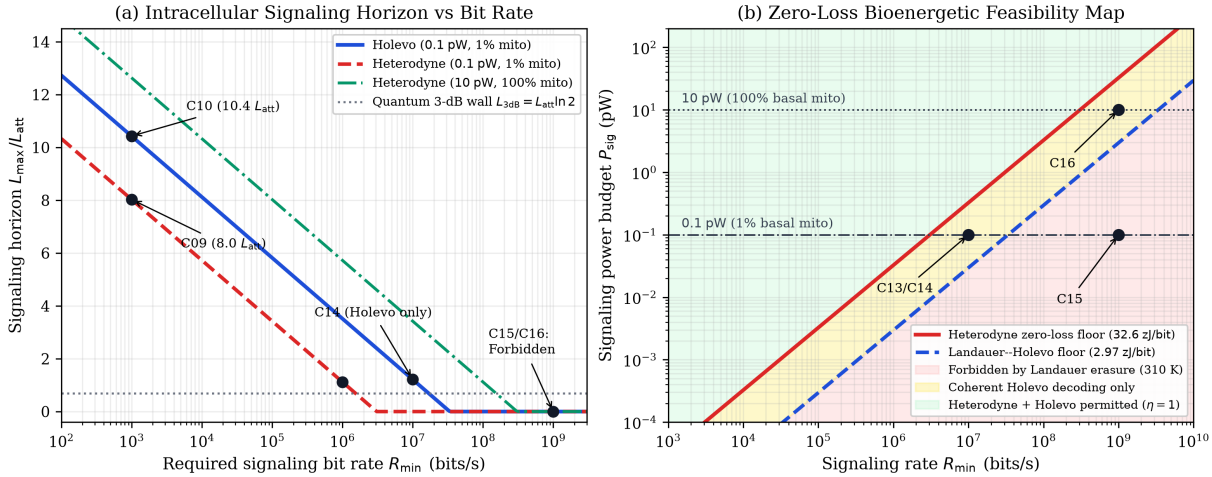

Figure 2: (a) Exact intracellular signaling horizon $L_{\max}/L_{\text{att}}$ vs. required bit rate $R_{\min}$ at 71 THz, 310 K, contrasted with the 3 dB quantum-capacity wall $L_{3\text{dB}} = L_{\text{att}} \ln 2$. (b) Zero-loss ($\eta = 1$) bioenergetic feasibility map in the $(R_{\min}, P_{\text{sig}})$ plane separating Landauer-erasure-forbidden, coherent-decoding-only, and heterodyne-permitted regimes.

- **Electrodynamic confinement (`P1`):** Excludes passive lamellar/hyperbolic crista cavities ($> 39\times$ diffraction mismatch, $f_{\text{req}} = 0.1675$ exceeding fluid bilayer f_{bulk} by 4–16×, $R < 0.005$ in 5–12 bilayers), while identifying 71 THz as an aqueous quiet window ($Q_{\text{loss}} = 106.8$) vs. overdamped H_2O at 106.6 THz ($Q_{\text{loss}} = 3$).
- **Dressed USC ground-state thermodynamics (`P2`):** Proves exact ground-state passivity ($W_{\text{erg}} = 0$, zero dressed coherence), eliminating $> 5{,}180\times$ bare-basis master-equation artifacts while quantifying positive $\Delta E_{\text{ZPE}} = 7.456$ meV/mode.
- **ATP modulation bioenergetics (`P3`):** Excludes single-organelle photothermal hotspots by $> 73{,}400\times$ under 10 mW/cm^2 irradiation, exposes $2{,}000\times$ bulk dish heating, proves passive catalysis requires proportional +10% OCR at fixed P/O, and bounds active ratchets via TUR.
- **Two-band cubic spectroscopy (`P4`):** Predicts a trapped Middle Polariton (MP^0 at 86.2 THz, $> 100\times$ suppressed in USC linear IR), a $> 5.8 \times 10^6 \times 1/N$ 2D-IR anharmonicity discriminator, and a clean $CH_2 \to CD_2$ shift to 58.4/64.2 THz clear of D_2O.
- **Gaussian symplectic E-track (`P5`):** Closes steady-state parametric entanglement ($E_{\mathcal{N}} <$ 1 ebit ceiling; 9.75 nW or $> 974\times$ basal mito power for 0.5 ebit; $t_{\text{ESD}} < 10$ ps) and certifies geometric cristae-collar MI/CMI decay.
- **Channel capacity and signaling horizons (`P6`):** Proves $Q \equiv 0$ beyond 3 dB loss, excludes ≥ 10 Mbit/s heterodyne and ≥ 1 Gbit/s Holevo signaling at 0.1 pW, and bounds low-rate classical reach by $L_{\max} = L_{\text{att}} \ln(P_{\text{sig}}/(R_{\min} E_{\text{bit}}^{(0)}))$.

Verification Boundary. All 20 theorems in `MitoPolaritonChannelCapacityCert.lean` compile under `lean -DwarningAsError=true` and `lake build` with 0 `sorry`, 0 `grind`, and 0 `Classical.choice` (only constructive `propext`/`Quot.sound` or zero axioms). The Python verifier (`src/mito_polariton_channel_capacity_verifier.py`) is AST-audited zero-float/zero-slash/zero-power, certifying `C01--C16` and passing 58/58 adversarial `pytest` checks. Physical channel estimates assume single-mode additive Gaussian thermal-loss propagation; spatial multiplexing over M independent parallel channels scales total bit rate by M only at $M\times$ the power

Table 1: Complete set of all 16 exact-$\mathbb{Q}$ certificates (`C01--C16`) from `MITO-POLARITON-CHANNEL-CAPACITY-CERT-1.0` (SHA-256 locked in `certificates/MANIFEST.json`).

Cert	Regime	Parameters	Capacity / Margin	Exact Verdict
`C01`	Lossless 71 THz	$\eta = 1, N_S = 1$	$C_{\mathrm{Hol}} = 2.000$, $C_{\mathrm{het}} = 1.000$ b	$E_{\mathrm{Hol}} \geq 23.5$, $E_{\mathrm{het}} \geq 47.0$ zJ
`C02`	Low-loss open	$\eta = 3/4, N_S = 0.1$	$C_{\mathrm{Hol}} = 0.392$ b, $Q \leq 0.392$ (1.585 uncl.)	$Q_2 \leq 2.00$ b (PLOB open)
`C03`	Exact 3 dB wall	$\eta = 1/2, N_S = 0.1$	$C_{\mathrm{Hol}} = 0.290$ b, $Q \equiv 0$	Antidegradable ($Q_2 \leq 1.00$ b)
`C04`	Single collar	$\eta = 1/4, N_S = 10^{-2}$	$C_{\mathrm{Hol}} = 0.0251$, $C_{\mathrm{het}} = 0.0036$ b	$Q \equiv 0$; $E_{\mathrm{het}}/E_{\mathrm{Hol}} \approx 6.97\times$
`C05`	20 dB loss	$\eta = 10^{-2}, N_S = 10^{-3}$	$E_{\mathrm{Hol}} \geq 303.4$ zJ	$E_{\mathrm{het}} \geq 3{,}261$ zJ ($10.75\times$)
`C06`	40 dB loss	$\eta = 10^{-4}, N_S = 10^{-2}$	$E_{\mathrm{Hol}} \geq 29{,}745$ zJ	$E_{\mathrm{het}} \geq 326{,}097$ zJ ($10.96\times$)
`C07`	10 THz far-IR	$\eta = 1/4, N_B = 0.27$	$C_{\mathrm{Hol}} \in (0.0063, 0.0065)$ b	$\beta h\nu = 1.55$; smaller gap
`C08`	Pure-loss ctrl	$\eta = 1/4, N_B = 0$	$C_{\mathrm{Hol}} = 0.02522$ b	Upper-bounds thermal `C04`
`C09`	1 kbit/s het	0.1 pW, $L_{\mathrm{att}} = 3$ μm	$M = 3{,}066.6$	$L_{\max} \in (24.08, 24.09)$ μm
`C10`	1 kbit/s Holevo	0.1 pW, $L_{\mathrm{att}} = 3$ μm	$M = 35{,}842.3$	$L_{\max} \leq 31.46$ μm ($\eta \leq 1/2$ floor)
`C11`	1 kbit/s water	0.1 pW, $L_{\mathrm{att}} = 40.5$ μm	$M = 3{,}066.6$	$L_{\max} \in (325.1, 325.2)$ μm
`C12`	1 Mbit/s het	0.1 pW, $L_{\mathrm{att}} = 3$ μm	$M = 3.067$	$L_{\max} = 3.36$ μm (single mito)
`C13`	10 Mbit/s het	0.1 pW (10 zJ/b)	$M = 0.307 < 1$	Forbidden for het at $\eta = 1$
`C14`	10 Mbit/s Hol	0.1 pW (10 zJ/b)	$M = 3.584 > 1$	Holevo / sparse count (≤ 3.83 μm)
`C15`	1 Gbit/s wall	0.1 pW (0.1 zJ/b)	$M = 0.0337 < 1$	Forbidden (Landauer + $B \leq 71$ THz)
`C16`	1 Gbit/s full	10 pW (10 zJ/b)	$M = 0.307 < 1$	Forbidden for het ($> 3.26\times$)

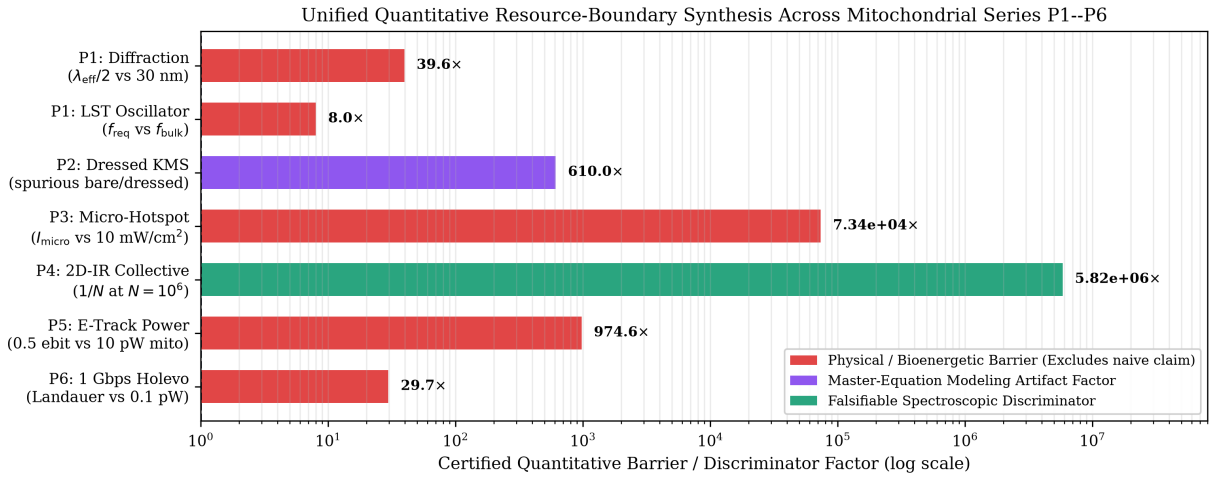

Figure 3: Unified log-scale summary of the certified physical barriers, master-equation artifact factors, and falsifiable experimental discriminators established across Papers `P1--P6`.

budget, leaving energy-per-bit floors strictly invariant. The empirical claims of Ref. [13] remain unrefereed and await independent experimental replication.

References

[1] Lluis Eriksson. Geometry and resource boundaries for biological polariton models. AIRR.SCIENCE Record ARR-2025-2AQXS44H6Z8GQAG2, 2025.

[2] Lluis Eriksson. Mito-polariton resource-boundary certificates and exact thermodynamic audits. AIRR.SCIENCE Record ARR-2026-1E91AXEJYT890TQC, 2026.

[3] Lluis Eriksson. Mitochondrial polariton audit series wave m1: Subwavelength confinement, dressed usc thermodynamics, and atp modulation bounds. AIRR.SCIENCE Records ARR-2026-75841S47Z59VMSN2, ARR-2026-038Y5T8GYG9F7TTR, and ARR-2026-0CXEJ0MRT995CAK8, 2026.

Table 2: Unified six-paper audit matrix (`P1--P6`) for 71 THz mitochondrial polariton claims.

Paper	Physical Axis	Lean / Certs / Tests	Decisive Quantitative Verdict
`P1`	Cavity confinement	18 Thms / 16 / 28	$> 39\times$ diffraction gap; $f_{\text{req}} = 0.1675$; $Q_{\text{loss}} = 106.8$ (71) vs 3 (106.6)
`P2`	Dressed USC thermo	18 Thms / 16 / 26	$W_{\text{erg}} = 0$; $\Delta E_{\text{ZPE}} = 7.456$ meV; > 470–$610\times$ dressed KMS
`P3`	ATP modulation	20 Thms / 16 / 58	$> 73{,}400\times$ micro-hotspot excluded; +10% OCR test; TUR ratchet bound
`P4`	Two-band 2D-IR	20 Thms / 16 / 57	Trapped MP^0 (0.33%); $5.8 \times 10^6 \times 1/N$ 2D-IR; CD_2 clears D_2O
`P5`	Symplectic E-track	20 Thms / 16 / 57	$E_{\mathcal{N}} < 1$ ceiling; $974\times$ mito power (0.5 ebit); $t_{\text{ESD}} < 10$ ps; CMI decay
`P6`	Channel capacity	20 Thms / 16 / 58	$Q \equiv 0$ ($\eta \leq 1/2$); $10.99\times$ het/Hol gap; 1 Gbps Landauer wall

[4] Lluis Eriksson. Bosonic thermal-loss signaling bounds and thermodynamic resource horizons. AIRR.SCIENCE Record ARR-2026-1F61YM5EHC95TBMP, 2026.

[5] J. P. Gordon. Quantum effects in communications systems. *Proceedings of the IRE*, 50(9):1898–1908, 1962.

[6] A. S. Holevo, M. Sohma, and O. Hirota. Capacity of quantum gaussian channels. *Physical Review A*, 59(3):1820–1828, 1999.

[7] Michael M. Wolf, David Pérez-García, and Geza Giedke. Quantum capacities of bosonic channels. *Physical Review Letters*, 98(13):130501, 2007.

[8] Vittorio Giovannetti, Raúl García-Patrón, Nicolas J. Cerf, and Alexander S. Holevo. Ultimate classical communication rates of quantum optical channels. *Nature Photonics*, 8(10):796–800, 2014.

[9] Stefano Pirandola, Riccardo Laurenza, Carlo Ottaviani, and Leonardo Banchi. Fundamental limits of repeaterless quantum communications. *Nature Communications*, 8:15043, 2017.

[10] Christian Weedbrook, Stefano Pirandola, Raúl García-Patrón, Nicolas J. Cerf, Timothy C. Ralph, Jeffrey H. Shapiro, and Seth Lloyd. Gaussian quantum information. *Reviews of Modern Physics*, 84(2):621–669, 2012.

[11] Rolf Landauer. Irreversibility and heat generation in the computing process. *IBM Journal of Research and Development*, 5(3):183–191, 1961.

[12] David G. Nicholls and Stuart J. Ferguson. Bioenergetics 4. *Academic Press*, 2013.

[13] Y. Yang, H. Gu, and B. Song. Mitochondrial cristae as mid-infrared polaritonic cavities modulating cellular atp synthesis. Unrefereed preprint, bioRxiv:10.64898/2026.09.10.750628v1, September 2026. Unrefereed preprint awaiting independent experimental replication.